Stem Cell Reports

Article

OPEN ACCESS

Long-term adherence of human brain cells *in vitro* is enhanced by charged amine-based plasma polymer coatings

Bridget Milky,[1,2] Michael Zabolocki,[1,2] Sameer A. Al-Bataineh,[3,6] Mark van den Hurk,[1] Zarina Greenberg,[1] Lucy Turner,[1] Paris Mazzachi,[1,2] Amber Williams,[1,2] Imanthi Illeperuma,[1] Robert Adams,[1,2] Brett W. Stringer,[1,2] Rebecca Ormsby,[2] Santosh Poonnoose,[2] Louise E. Smith,[3,5,6] Marta Krasowska,[5] Jason D. Whittle,[4,6] Antonio Simula,[3,6] and Cedric Bardy[1,2,*]

[1]South Australian Health and Medical Research Institute (SAHMRI), Laboratory for Human Neurophysiology and Genetics, Adelaide, SA, Australia

[2]Flinders University, Flinders Health and Medical Research Institute (FHMRI), College of Medicine and Public Health, Adelaide, SA, Australia

[3]TekCyte Limited, Adelaide, SA, Australia

[4]University of South Australia STEM, Mawson Lakes Campus, Mawson Lakes, SA, Australia

[5]Future Industries Institute, University of South Australia STEM, Mawson Lakes Campus, Mawson Lakes, SA, Australia

[6]Cooperative Research Centre for Cell Therapy Manufacturing (CTM CRC), Adelaide, SA, Australia

*Correspondence: cedric.bardy@sahmri.com or cedric.bardylab@gmail.com (C.B.)

https://doi.org/10.1016/j.stemcr.2022.01.013

SUMMARY

Advances in cellular reprogramming have radically increased the use of patient-derived cells for neurological research *in vitro*. However, adherence of human neurons on tissue cultureware is unreliable over the extended periods required for electrophysiological maturation. Adherence issues are particularly prominent for transferable glass coverslips, hindering imaging and electrophysiological assays. Here, we assessed thin-film plasma polymer treatments, polymeric factors, and extracellular matrix coatings for extending the adherence of human neuronal cultures on glass. We find that positive-charged, amine-based plasma polymers improve the adherence of a range of human brain cells. Diaminopropane (DAP) treatment with laminin-based coating optimally supports long-term maturation of fundamental ion channel properties and synaptic activity of human neurons. As proof of concept, we demonstrated that DAP-treated glass is ideal for live imaging, patch-clamping, and optogenetics. A DAP-treated glass surface reduces the technical variability of human neuronal models and enhances electrophysiological maturation, allowing more reliable discoveries of treatments for neurological and psychiatric disorders.

INTRODUCTION

Human induced pluripotent stem cells (hiPSCs) and advances in cell reprogramming technologies have created new opportunities for pre-clinical research (Ebert et al., 2012; Hamazaki et al., 2017) by providing *in vitro* access to virtually any type of human cell (Ebert et al., 2012; Mertens et al., 2016; Rowe and Daley, 2019; Sarkar et al., 2018; Vadodaria et al., 2016). Pre-clinical patient-derived hiPSC models are especially valuable for the study of neuronal tissue, which is otherwise challenging or unethical to obtain from human brain biopsies (Parr et al., 2017).

Reprogrammed brain tissue is generated in Petri dishes as adherent cell cultures or non-adherent organoids (Lancaster et al., 2013). Despite recent progress in the development of non-adherent organoid models (Di Lullo and Kriegstein, 2017; Kim et al., 2020), adherent cultures largely remain the standard of choice for neuronal research *in vitro*. Adherent cultures offer greater reproducibility and higher-throughput screening capabilities over non-adherent systems (Duval et al., 2017; Liu et al., 2018) and provide easier access for a range of assays, including imaging and electrophysiology (Bardy et al., 2015; Liu et al., 2018). However, maintaining long-term cell adhesion is often a technical challenge in post-mitotic neuronal cultures. This is particularly problematic for human neurons, which require significantly longer periods than animal primary neurons to mature and establish synaptic circuits *in vitro* (Bardy et al., 2016; Ray et al., 2014). With these long timeline requirements, issues of detachment and aggregation are common, and solutions are limited.

It is widely known that neurons adhere better to plastic (tissue culture-treated polystyrene [TCPS]) substrates than standard glass; here, we demonstrate this experimentally for the first time. However, growing neurons on transferable glass coverslips remains necessary for most patch-clamping and functional imaging assays. Glass coverslips provide several advantages: (1) transferability into imaging/electrophysiology setup for acute experiments, (2) optimal optical properties, and (3) optimal weight/buoyancy, which improves the physical stability of cells for patch-clamping or live imaging *in vitro*. Therefore, we investigated whether plasma polymer surfaces could sustain the adhesion of human brain cells on glass similar to or better than TCPS for long-term functional maturation. We also tested their effectiveness in combination with various extracellular matrix (ECM) components or attachment factors.

Previous research efforts have focused mainly on improving the surface attachment of non-neuronal cell types (Hamerli, 2003; Lakard et al., 2004) or tethering growth factors to polystyrene cultureware (Gomez et al., 2007; Gomez and Schmidt, 2007; Granato et al., 2018;

Hamazaki et al., 2017; Leipzig et al., 2009). Cultureware currently used in neuroscience research was not designed to support the long-term adhesion of functional human neurons, and the specific biomaterial characteristics required are unknown.

We performed our experiments on modified glass coverslips and identified diaminopropane (DAP) plasma polymer treatment with a laminin-based coating to optimally support neuronal culture adhesion. We found that DAP-laminin treatments increase the adhesion of human neurons and astrocytes on glass for as long as 27 weeks and support their viability and electrophysiological properties. We also show that this treatment improves the adhesion of a range of human proliferating neuronal cell types, including neural/glia progenitors and brain tumor cells.

RESULTS

Neuronal cell cultures detach from standard glass surfaces sooner than from tissue culture polystyrene

Neuronal culture adhesion is influenced by the cultureware properties, which can be modified with chemical treatments and ECM coatings (Figure 1A). To quantify the extent of neuronal detachment from the cultureware, we matured human neural progenitor cells (NPCs) to neurons and astrocytes on TCPS (plastic) or standard glass coverslips (Figure 1B). Detachment was determined using the total area where cells were no longer present on the surface (Figures 1C and 1D). All tested ECM proteins and polymeric attachment factors failed to completely prevent progressive detachment on standard glass. For all ECM and polymeric factors tested on glass, <50% of the culture remained after 5 weeks. The lowest detachment on standard glass was observed after pre-coating for 24 h with laminin and poly-ornithine (PLO-Lam; Figure 1E).

In contrast, TCPS (with PLO-Lam) supported cell attachment longer than standard glass (with PLO-Lam). Despite variability in cell attachment between neuronal batches, TCPS superiority was consistent over multiple ($n = 6$) independent experiments (Figure 1F; $p = 0.0317$). On average, the first sign of detachment commenced after 1 week for cultures on standard glass and 5 weeks on TCPS. Detachment continued steadily over time and was much more prominent on standard glass (Figure 1F). Neuronal detachment may occur on any type of substrate, as it strongly depends on the quality of the cells and experimenter handling. However, TCPS clearly supports long-term cell adhesion better than standard glass. To exemplify the importance of long-term culture for electrophysiological maturation of human neurons *in vitro*, we measured the progression of network bursting and synchronous communication of hPSC-derived midbrain neuronal cultures. Neuronal cultures required up to 9 weeks of maturation before exhibiting network bursting and synchrony, and these properties continued to increase until at least 13 weeks in culture (Figures 1G and 1H). Therefore, cultureware that does not support neuronal adherence for extended periods (>13 weeks) is suboptimal for studies requiring electrophysiologically mature neurons.

Composition of plasma monomers determined by X-ray photoelectron spectroscopy (XPS)

To investigate the advatanges of various plasma treatments for the long-term culture of neuronal cells, we deposited on the cultureware surface a range of ultrathin plasma polymer films, prepared from their respective monomers. We tested allylamine (AAM), DAP, heptylamine (HA), acrylic acid (AAC), octadiene (OD), and AAM with a layer of heparin adsorbed (AAM-H). The optimized plasma parameters for the high retention of functional groups on the generated plasma polymer films are listed in Table S1. These functional groups include amine (in AAM, DAP, and HA), carboxylic (in AAC), and hydrocarbon (in OD). We measured the plasma film thickness using a quartz crystal microbalance. Thicknesses ranged from 33 to 54 nm, and the computed deposition rates ranged between 0.8 and 3.6 nm/min (Table S1). Film properties and elemental compositions reported in this study are consistent with those reported previously (Kirby et al., 2017; Smith et al., 2016).

Specific plasma polymer treatments improve neuronal cell adhesion on glass surfaces

We examined six plasma-treated glass surfaces generated for their ability to promote cell adhesion in comparison to glass without plasma treatment (standard glass) and TCPS cultureware. DAP and AAM polymer films on glass significantly outperformed standard glass or other plasma treatments (HA, OD AAC, and AAM-H) over multiple independent experiments ($n = 3–6$) (Figures 2A–2C). The detachment progression over 13 weeks of neuronal cultures on glass-DAP, glass-AAM, and TCPS was minimal compared to standard glass (Figure 2B). Overall, at 13 weeks, glass-DAP showed the highest mean attachment (96%) compared to the next 2 best surfaces (glass-AAM, 92%; TCPS, 90%) and substantially outperformed all of the other surfaces (Figures 2A, 2C, and S1A–S1D; Table S2). This demonstrates that specific thin-film plasma polymer treatments on glass (DAP or AAM) significantly improve cell adhesion to a level comparable to TCPS.

The physicochemical properties of plasma polymer surfaces contribute to their adhesion-promoting capability

To understand the connection between the chemical properties of the plasma polymerized surfaces and their ability

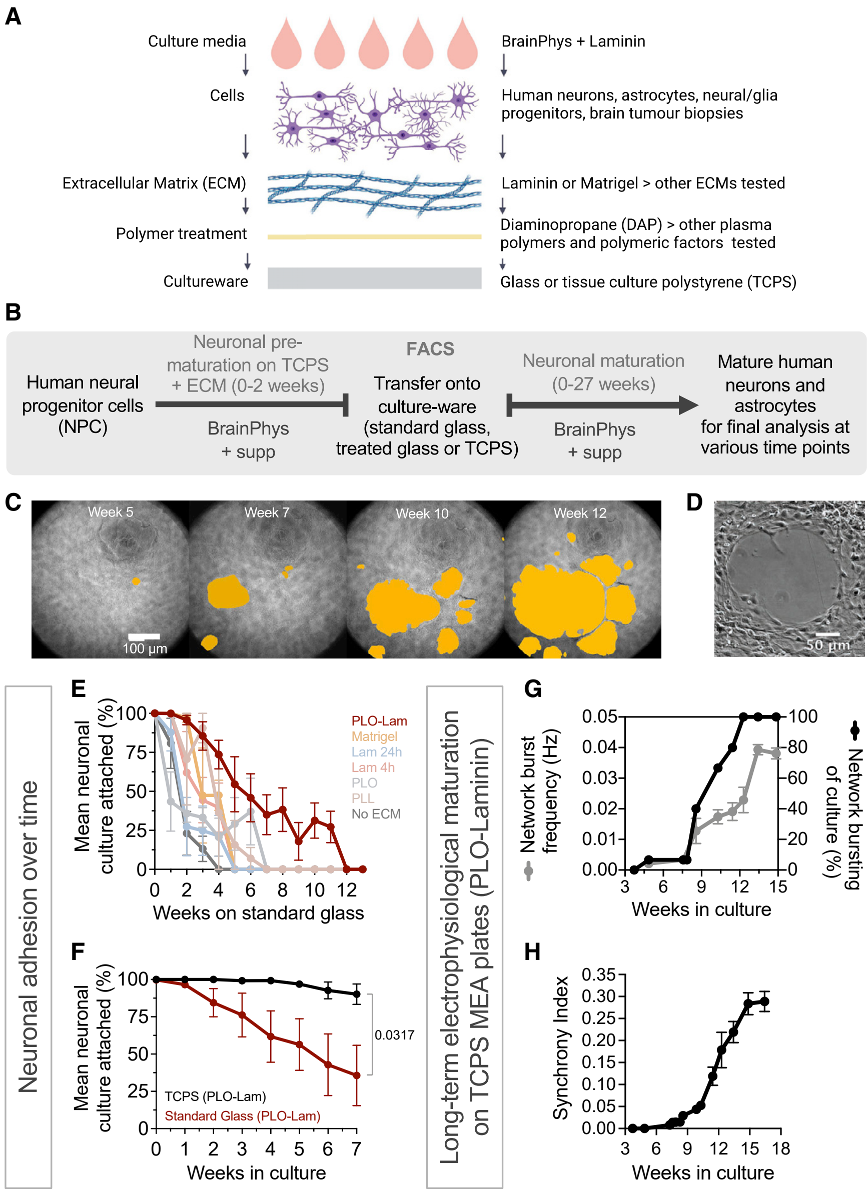

Figure 1. Neuronal cells detach from standard glass surfaces sooner than from tissue culture polystyrene

(A) Schematic of the cell culture microenvironment and modifications tested to improve neuronal attachment.

(B) Human neural progenitor cells (NPCs) were pre-matured in BrainPhys + supplements for 0–2 weeks, replated on test surfaces, and further matured for up to 27 weeks in BrainPhys + supplements before phenotypic analyses. Before replating on test surfaces, post-mitotic precursors were sorted for DAPI exclusion at 2 weeks (see Experimental procedures).

(C and D) Live neuronal cultures under phase contrast at 4× and 20× magnification, respectively. Detachment was quantified from 4× magnification phase contrast images by tracing regions with no cells (yellow) and calculating their combined area as a fraction of the total field of view area for each well.

(E) Detachment on standard glass across multiple coating solutions: poly-L-ornithine (PLO; n = 4), PLO-laminin (Lam) (n = 6), Matrigel (n = 2), 24 h treatment of laminin (n = 6), 4 h treatment of laminin (n = 2), uncoated (n = 6), and poly-L-lysine (PLL; n = 2); n replicates from 2 independent experiments, means ± SEMs represented.

(F) Cell detachment on standard glass compared to plastic (TCPS) both with PLO-Lam. Means ± SEMs from n = 5 biologically independent experiments, 2–6 replicates per experiment.

(G and H) Spontaneous multi-electrode array (MEA) recordings of hPSC-derived neuronal cultures showing network burst activity and synchrony over 15–17 weeks on TCPS plates pre-coated with PLO-Lam. Means ± SEMs data from 16 replicate wells, each well containing 16 electrodes.

to promote neuronal adhesion, we performed XPS analyses on the monomers used for plasma treatments and the thin film of polymers on the glass surfaces. Among the monomers used for the plasma treatments, DAP monomer contained the greatest number of primary amine groups and nitrogen:carbon ratio, followed by AAM and HA (Figure 2E). We also confirmed that the monomer nitrogen:carbon ratios were conserved on the polymer films applied to glass (Figures 2E–2G). The polymers containing amine groups (DAP, AAM, and HA) outperformed the non-aminated polymers tested (e.g., AAC, OD), demonstrating the importance of amine groups for neuronal adherence. We then asked whether the hydrophobicity of the surface could influence neuronal adhesion. We found that the hydrophobicity of the most performant polymers (DAP and AAM) had a contact angle of water in the medium range (~60°), suggesting that increasing or decreasing the hydrophobicity alone is not sufficient to improve neuronal adhesion (Figure 2H). We then asked whether the electrical charge of the surfaces could influence neuronal adhesion. We measured the zeta potential of the polymer-treated glass surfaces and found a significant linear correlation ($p = 0.01$; $R^2 = 0.90$) between the electrical charge and neuronal adhesion (Figure 2I). The most neuronal adherent surface,

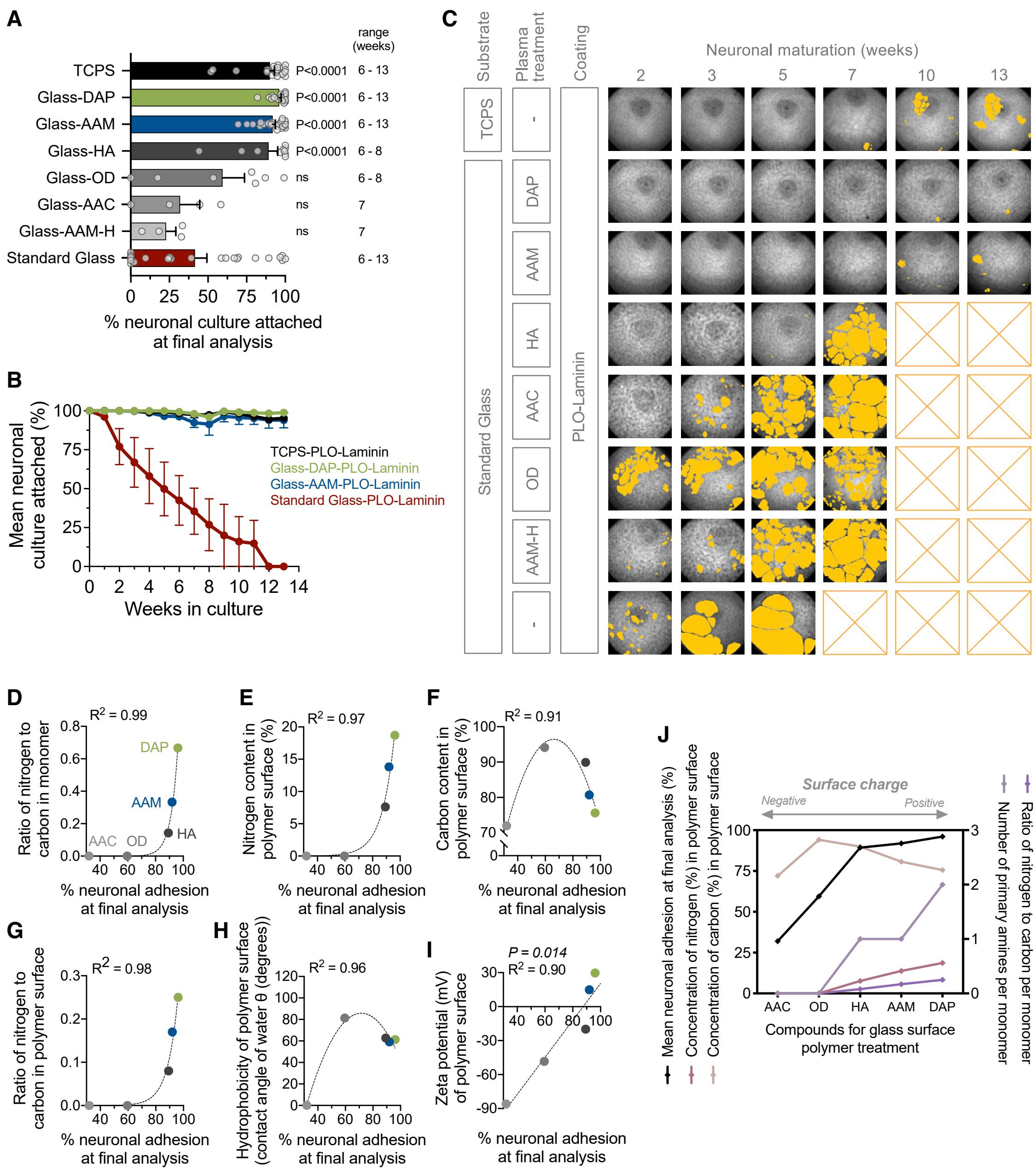

Figure 2. Positively charged amine-terminated plasma polymer treatments improve long-term neuronal attachment on glass

(A) Detachment of neuronal cultures on plasma polymer-treated glass surfaces, diaminopropane (glass-DAP; n = 18, N = 6), allylamine (glass-AAM; n = 26, N = 7), heptylamine (glass-HA; n = 10, N = 3), octadiene (glass-OD; n = 7, N = 2), acrylic acid (glass-AAC; n = 4, N = 1), or allylamine with added heparin (glass-AAM-H; n = 4, N = 1), compared to standard glass (n = 26, N = 7) and plastic (TCPS; n = 22, N = 6). n replicates wells/coverslips across N independent experiments. Means (±SEMs) attachment percentages at termination of experiment (range, 6–13 weeks). Significance determined using Mann-Whitney tests.

(B) Detachment of neuronal cultures on glass-AAM, glass-DAP, standard glass, and TCPS, all with PLO-Lam. Means (±SEMs) values (0–7 weeks, n = 4–6 independent experiments with 2–6 replicates per experiment; 8–13 weeks, n = 2 independent experiments with 2–4 replicates per experiment).

(C) Phase contrast images at 4× magnification of representative wells per condition. Yellow regions indicate detached cell culture, and crossed boxes indicate complete detachment.

(D–J) X-ray photoelectron spectroscopy (XPS) results of monomer and polymer composition of AAC, AAM, DAP, HA, and OD, shown against mean neuronal adhesion at the final time point analyzed. Data shown as means ± SEMs. Dotted line indicates line of best fit. (D) Ratio of

(legend continued on next page)

glass-DAP, had the highest potential, at ~30 mV (measured in phosphate-buffered saline [PBS] at physiological pH). These results demonstrate that the properties of the plasma polymer film can determine the neuronal adhesion capability. In particular, positively charged, amine-terminated, hydrophilic plasma polymerized surfaces best support neuronal adhesion on cultureware (Figure 2J).

Laminin-based ECM coating is required for long-term neuronal adhesion on glass-DAP

To determine the optimal fresh ECM coating required before seeding neuronal cells on DAP-treated glass, AAM-treated glass, and TCPS, we evaluated six common polymeric/ECM adhesive factors (Figures 3A and 3B). The performance of glass-DAP and glass-AAM surfaces remained comparable to that of TCPS regardless of the polymeric/ECM adhesive factors added. The laminin protein network forms the major component at the foundation of the ECM for most tissue, including brain cells (Mouw et al., 2014; Nirwane and Yao, 2018). We found laminin-based coatings on glass-DAP and TCPS necessary for long-term neuronal adherence (Figures 3A and 3B). Although adding polymeric factor PLO to the laminin coat slightly improved cell adhesion on standard glass (Figure 1E), it did not have any apparent benefit when using glass-DAP (Figures 3A and 3B). Coating glass-DAP (or TCPS) with laminin for 24 h rather than 4 h improved adhesion over extended culture periods (>8 weeks) (Figures 3A and 3B). In conclusion, pre-coating TCPS, glass-DAP, and glass-AAM with either laminin for 24 h or Matrigel was required to support >90% adhesion of human neuronal culture for >13 weeks in BrainPhys maturation medium (Figures 3A and 3B).

DAP-treated glass surfaces improve the adherence of proliferative brain-specific cells

Neural (NPCs) or glia progenitor cells (GPCs) usually proliferate in culture to reach confluency within ~1 week and, as such, do not usually require long-term adhesion. However, to optimize live or post-fixation imaging assays, these cells are often cultured on glass surfaces. Therefore, we assessed whether proliferating neural stem cells or glia cells could be cultured on glass-DAP. We compared the proliferation rate of three human proliferative brain cell types: GPCs and NPCs (stem cell-derived) and glioblastoma tumor cells (GBMs; obtained from a brain cancer patient) on glass-DAP, TCPS, and standard glass. All of the surfaces were pre-coated for 1 h with fresh Matrigel just before seeding. Despite initially seeding the exact same number of cells, 8 days later, we found significantly more cells (DAPI + after fixation) on glass-DAP than standard glass for all neuronal cell types (NPCs, GPCs, and GBMs) (Figures 4A–4D). We found no significant difference (Figures 4B and 4C) or a small benefit (Figure 4A) of glass-DAP compared to TCPS. These results demonstrate that DAP treatment optimizes the shorter-term (~8 days) culture of a range of proliferative neuronal cells on glass.

We then tested the adherence of proliferating non-neuronal human embryonic stem cells (hESCs) on the same three surfaces. In contrast with the proliferating neuronal cells, TCPS appeared to support the proliferation of stem cells better than glass-DAP. The stem cells formed three-dimensional (3D) colonies, which challenged the accurate DAPI nuclei counts, but more cells were visible on TCPS (Figure 4F). The area covered by the colonies was also significantly larger in TCPS than glass-DAP, and the smallest was on standard glass (Figure 4E). Therefore, glass-DAP may also support the short-term culture of stem cells better than standard glass; but TCPS or other more specialized polymers may be preferred for non-neuronal application.

DAP-treated glass surfaces improve adhesion compared to standard glass while maintaining neuronal cell viability

We identified that DAP-laminin-treated glass was the optimal choice to reduce human neuronal culture detachment (Figures 2 and 3). To determine whether such improvement was mediated by increased cell adhesion or cell survival, we performed a viability assay on human neuronal cultures after 9 weeks on TCPS, standard glass, glass-DAP or glass-AAM. Over time, we did not observe an increase in lactate dehydrogenase release in the supernatant in any conditions, suggesting a similar low cell-stress level on all substrates (Figure 4G). Despite fewer cells adhering to standard glass after 9 weeks in culture, proportions of live/dead cells on the various surface conditions were comparable (Figures 4H and S2). These results support the fact that DAP treatment improves adhesion without impairing cell viability.

nitrogen:carbon in monomer (exponential growth, $R^2 = 0.99$). (E and F) Content of nitrogen (exponential growth, $R^2 = 0.97$) (E) and (F) carbon (second-order polynomial, $R^2 = 0.91$) in the polymer as a percentage of total atoms. (G) Ratio of nitrogen:carbon in the polymer surface derived from AAC, AAM, DAP, HA, and OD monomers (exponential growth, $R^2 = 0.98$). (H) Advancing contact angle of water on AAC, AAM, DAP, HA, or OD polymer surfaces (second-order polynomial, $R^2 = 0.96$); 30 replicate measurements per surface to calculate means ± SEMs. (I) Zeta potential (mV) of the resulting polymer film (linear regression, slope = 1.63, $R^2 = 0.90$, p = 0.014). (J) Summary of XPS results for AAC, AAM, DAP, HA, and OD monomers and polymers, and mean culture adhesion at final analysis.

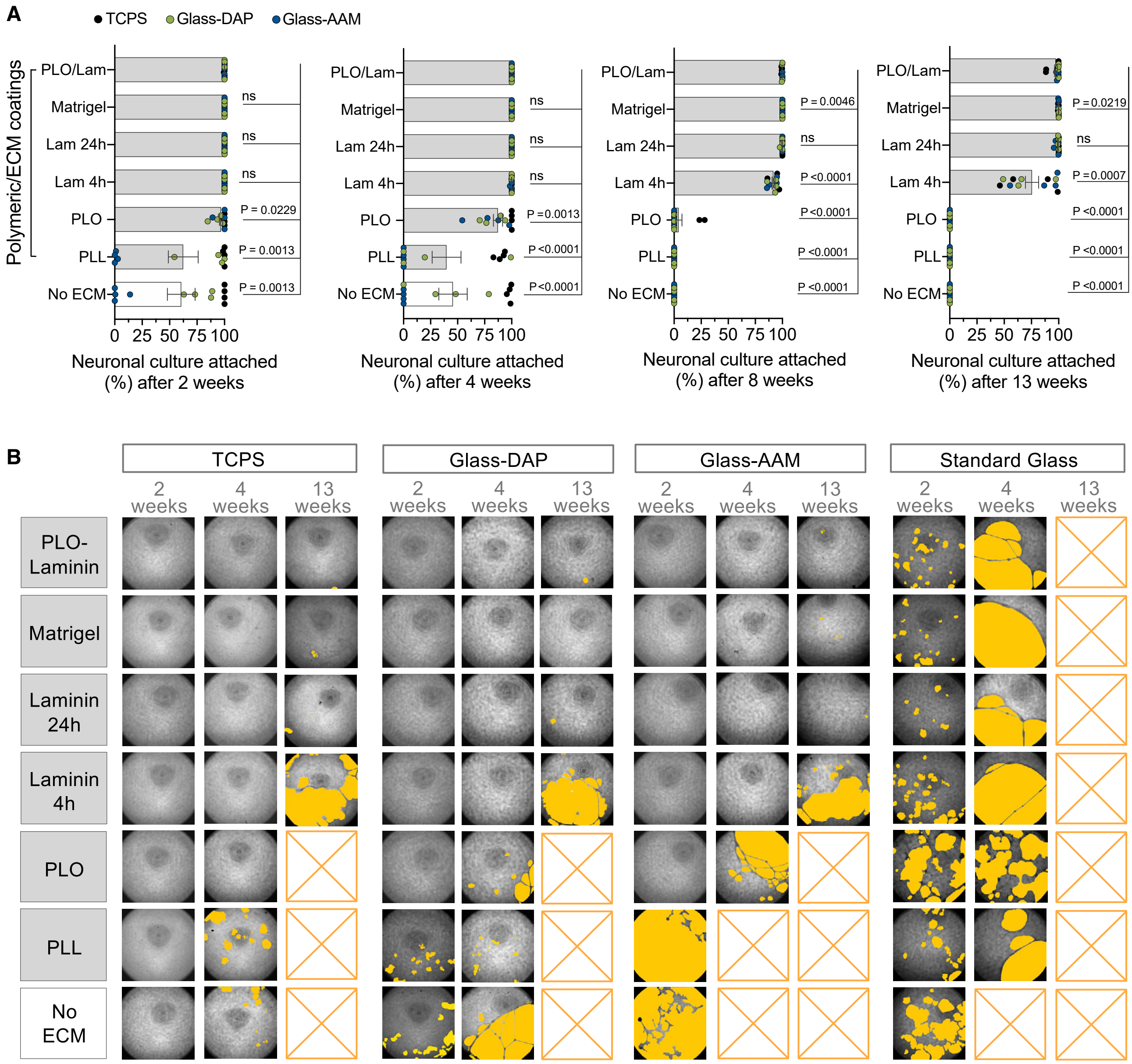

Figure 3. Laminin-based ECM coatings improve long-term neuronal attachment on TCPS and glass-DAP

(A) Detachment of neuronal cultures on surfaces (TCPS, glass-DAP or glass-AAM) pre-coated with various polymeric/extracellular matrix (ECM) solutions: PLO/LAM, Matrigel, 24 h laminin treatment (LAM 24 h), 4 h laminin treatment (LAM 4 h), PLO, polylysine (PLL), and no additional coating (no ECM). Means (±SEMs) percent attachment at 2, 4, 8, and 13 weeks in maturation medium; n = 12 replicates from 2 independent experiments.

(B)Phase contrast images at 4× magnification of representative wells per polymeric/ECM condition on treated surfaces at 2, 4, and 13 weeks in culture. Yellow regions indicate detached cells; crossed boxes indicate complete detachment.

DAP-treated glass surfaces support the adhesion of mature neurons and astrocytes

hPSC-derived neuronal culture comprises a mixture of neurons and astrocytes, which is essential for establishing synaptic circuits. We found that glass-DAP with laminin supports the maturation of both astrocytes (GFAP^{+} [glial fibriallary acidic protein positive]) and neurons (MAP2^{+} [microtubule-associated protein 2 positive]) and the formation of complex dendritic networks and synaptic contacts (SYN^{+} [s$^{\text{ynapsin I}}$]) (Figures 4I and 4J). To determine whether DAP treatment affected the astrocyte:neuron ratio in culture, we used lentiviral vectors and promoter-driven fluorescent proteins to quantify the proportion of live neurons (synapsin:GFP) and astrocytes (GFAP:tdTomato) with flow cytometry.

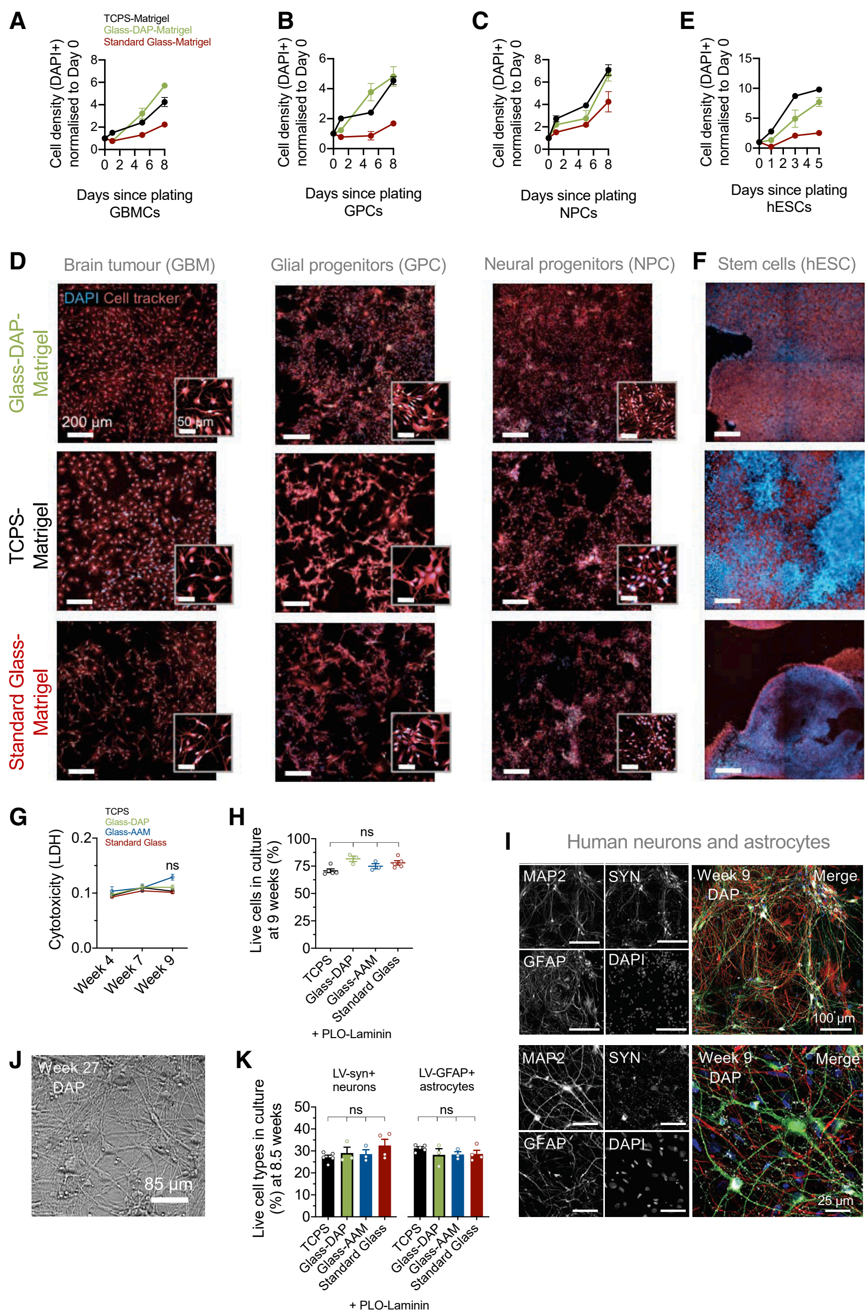

Figure 4. DAP-treated glass surface supports human proliferative neuronal/glia progenitors, brain tumor cells, and post-mitotic mature neurons and astrocytes

(A–D) Analysis of proliferative human brain cells on various substrates. Attachment determined by counting fixed nuclei ($DAPI^+$) over time. Means ± SEMs fold change in number of nuclei per well (normalized to day 0) calculated for 5–6 replicate wells/condition/time point (1 independent experiment). All of the surfaces were pre-coated with Matrigel. Proliferative human brain cells analyzed were (A) patient-derived glioblastoma tumor cells (GBMs), (B) hESC-derived glial precursor cells (GPCs), and (C) hESC-derived neural progenitor cells (NPCs). (D) Immunofluorescence staining of DNA (DAPI; blue) and cell soma (CellTracker, red) at latest time point (8 days for brain cells). See also Figure S3.

(E) Proliferation of non-neuronal human embryonic stem cells (H9, hESC) was measured as the fraction of area covered by colonies normalized to day 0 (n = 5–6 replicates from 1 independent experiment).

(F) Immunofluorescence staining of DNA (DAPI; blue) and cell soma (CellTracker, red) at latest time point (5 days for stem cells). See also Figure S3.

(G and H) Cytotoxicity analysis of neuronal cultures. All of the surfaces were pre-coated with PLO-Lam. (G) Lactate dehydrogenase (LDH) relative concentrations measured in neuronal culture supernatant (n = 15 replicates from 5 independent experiments) to estimate cellular stress. (H) Without fixation, DNA marker DAPI is incorporated in the nuclei of dead or dying cells ($DAPI^+$), but not live cells ($DAPI^-$). Means ± SEMs proportions of live cells ($DAPI^-$).

(I) Immunofluorescence staining of MAP2, GFAP, and synapsin at 10× magnification (top) and 40× magnification (bottom) in neuronal cultures after 9 weeks in maturation medium, on glass-DAP-LAM.

(J) Live neuronal cultures on glass-DAP-LAM under phase contrast at 20× after 27 weeks in maturation medium.

(K) FACS analysis of the proportion of neurons (Lv-synapsin-GFP) and astrocytes (Lv-GFAP-tdTomato) at 9 weeks in maturation medium on different surfaces.

For (H) and (K), n = 3–5 replicates per condition from 2 independent experiments. p values calculated using Mann-Whitney tests, ns for $p > 0.05$.

Despite fewer cells on standard glass, the astrocyte: neuron ratio remained constant between all of the surfaces tested (Figure 4K). These results demonstrate that DAP-laminin coating supports the maturation of complex neuronal/astrocytic circuits.

Positively charged DAP coating does not impair neuronal membrane excitability and supports long-term electrophysiological maturation

The electrical activity of human neurons is integral to their development and function. We demonstrated that a

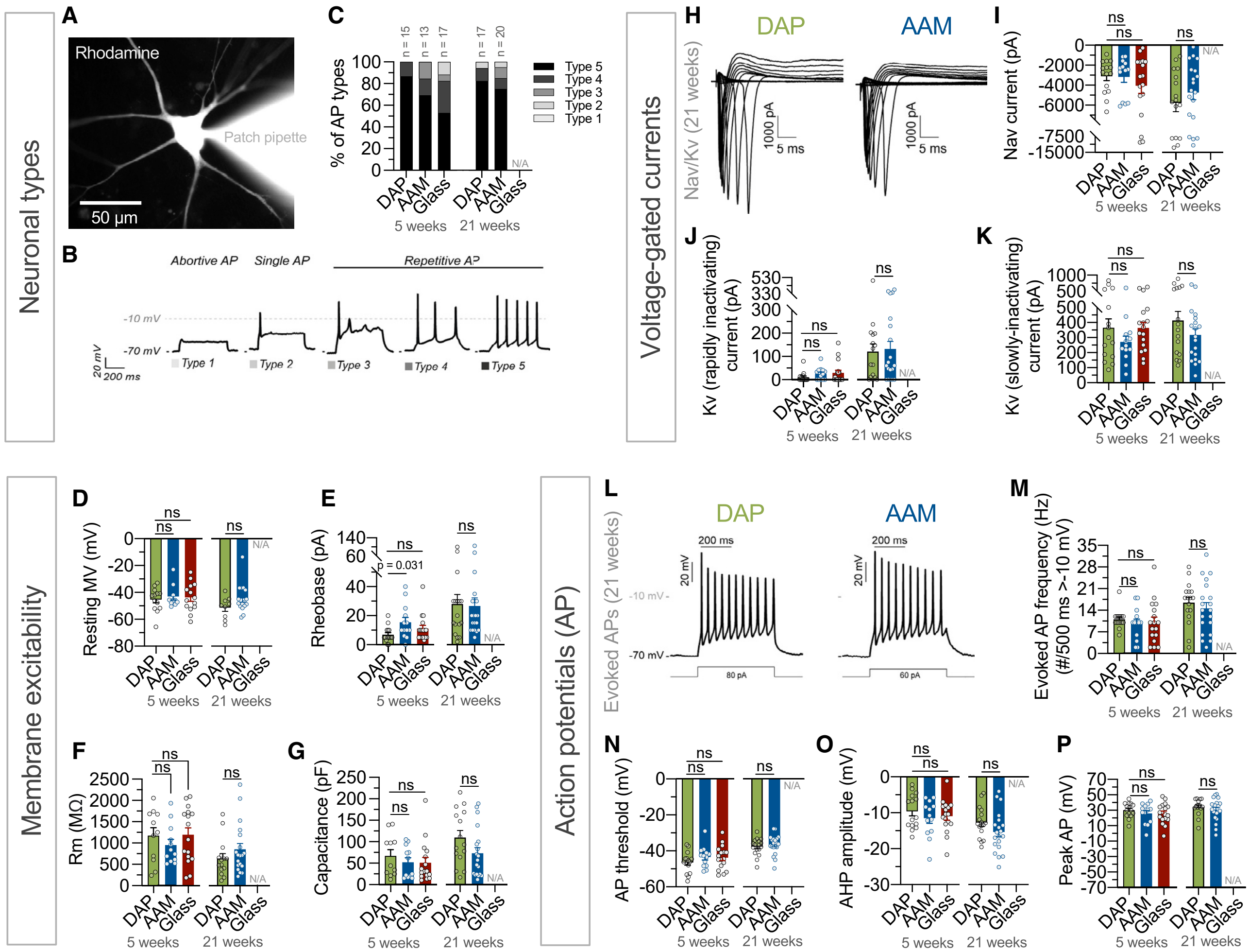

Figure 5. Positively charged DAP coating does not impair neuronal membrane excitability and supports the fundamental electrophysiological functions of human neurons *in vitro*

Whole-cell patch-clamp recordings from hPSC-derived midbrain neurons at 5 or 21 weeks. All surfaces (glass-DAP [DAP], glass-AAM [AAM], standard glass [glass]) were pre-coated with PLO-Lam. Data from standard glass were not obtained at 21 weeks due to substantial detachment (see Figures 1, 2, 3, and 4).

(A) Representative image of a rhodamine-filled patch-clamped neuron on glass-DAP at 21 weeks (148 days) in maturation medium.

(B) Example action potential (AP) type classifications (based on Bardy et al., 2016).

(C) AP type quantification of neurons (n = 82 neurons) patch-clamped across 22 coverslips at 5 and 21 weeks.

(D–G) Neuronal membrane excitability on test surfaces. (D) Resting membrane potentials (mV) measured from neurons on glass-DAP (n = 13 + 9), glass-AAM (n = 10 + 16), and standard glass (n = 14) at 5 and 21 weeks, respectively. (E) Rheobase of human neurons on glass-DAP (n = 15 + 17), glass-AAM (n = 13 + 20), and standard glass (n = 17). (F and G) Membrane resistance and capacitance of human neurons, measured on glass-DAP (n = 11 + 15), glass-AAM (n = 12 + 19), and standard glass (n = 16) at 5 and 21 weeks, respectively.

(H) Example voltage-clamp recordings from neurons on glass-DAP and glass-AAM over 21 weeks, held at −70 mV with +5 mV 500-ms depolarization steps.

(I–K) Voltage-gated currents of neurons on glass-DAP (n = 15 + 16), glass-AAM (n = 13 + 19), and standard glass (n = 17) at 5 and 21 weeks, respectively. (I) Peak voltage-gated sodium (Nav) currents. (J) Amplitudes of rapidly inactivating voltage-gated potassium (Kv) currents following the largest Nav current. (K) Amplitudes of slow inactivating Kv currents at −10 mV.

(L) Evoked AP example traces (type 5) at 21 weeks on glass-DAP and glass-AAM following a 500-ms depolarizing current step.

(M) Maximum firing frequencies (only APs reaching >−10 mV were selected).

(N) AP activation thresholds.

(O) After-hyperpolarization (AHP) amplitudes measured between the AP threshold potential and the lowest potential following the AP peak.

(legend continued on next page)

positively charged amine-terminated surface (+30 mV) improves neuronal adhesion (Figure 2). However, it is unknown whether the positive charge influences neuronal excitability. To address this, we performed whole-cell patch-clamp recordings of hPSC-derived neurons after maturing for 5 weeks (n = 45 neurons) or 21 weeks (n = 37 neurons) on glass-DAP, glass-AAM, and standard glass (Figure 5). All of the surfaces were pre-coated with PLO-Lam for 24 h and cultured in BrainPhys maturation medium. TCPS is suboptimal for electrophysiology *in vitro* due to low optical quality (high refractive index) and higher buoyancy in saline solution (reduces the physical stability required for patch-clamping). Therefore, glass coverslips are considered the gold standard for electrophysiology *in vitro*, and we did not test neuronal functionality on TCPS. Human neurons expressing synapsin:GFP and displaying clear neuronal morphology and dendritic arborizations were patch-clamped (Figure 5A). In current-clamp, cells were held at −70 mV and injected with incremental current steps to evoke action potentials (APs), then categorized into 1 of 5 different neuronal types, depending on their firing frequencies (>−10 mV) defined in our previous study (Bardy et al., 2016) (Figure 5B). Glass-DAP supported a greater proportion of highly functional type 5 neurons at 5 weeks (87%) compared to glass-AAM (69%) and standard glass (53%) (Figure 5C), suggesting that glass-DAP better supports the adhesion of mature neurons. This trend continued at 21 weeks, where glass-DAP supported the highest proportion of type 5 neurons and the lowest proportion of low-functional neurons (types 1–3) (Figure 5C). Consistent with normal neurodevelopment trajectories, the membrane excitability, voltage-gated currents, and AP firing properties significantly matured between 5 and 21 weeks on glass-DAP (Figures 5D–5P). At the earlier time point (5 weeks), when compared to standard glass, we did not observe any significant influence of DAP treatment on membrane excitability, voltage-gated currents, or AP properties (Figures 5D–5P). At the latest time point (21 weeks), neuronal cultures on standard glass could not be recorded due to substantial detachment, but neither DAP or AAM treatments appeared to affect the neuronal membrane excitability, voltage-gated currents, or AP properties negatively (Figures 5D–5P).

We reported that supplementing PLO to the laminin precoating improved attachment on standard glass coverslips (Figure 1E), but it did not further improve the attachment on glass-DAP (Figure 3A). To avoid any bias, we compared the electrophysiology of neurons with PLO-Lam coating on all glass surfaces (Figures 5 and 6). However, we confirmed that the coating of laminin without PLO on glass-DAP was sufficient to support long-term electrophysiological maturation for >24 weeks (Figure S4B).

These results demonstrate that cultureware treatment with a thin film of positively charged DAP polymer and laminin does not influence the resting membrane potential or excitability of the neurons. Standard glass with PLO-Lam may be used for electrophysiological assays at early time points, but is suboptimal for the longer period required for functional maturation. Instead, glass-DAP-LAM optimally supports patch-clamping of neurons maturing for periods as long as ≥21 weeks.

DAP-LAM surfaces promote the maturation of synaptically active neural networks

We demonstrated that DAP-treated coverslips optimally support the excitability of single neurons (Figure 5). However, it is unknown whether DAP surfaces also support the formation of neurite arborization and synaptic networks. To address this, we immunostained hPSC-derived neuronal cultures on glass-DAP, glass-AAM, and standard glass coverslips (Figures 6A–6D). To avoid bias due to partial detachment, we used an automated high-content confocal detection system to image only the fields of view with similar MAP2$^+$ neuron density and avoided analysis of the regions where cells had detached. We confirmed that adhesion after fixation and density of neurons remained similar between the field of views selected for morphological analysis (Figures S4C–S4E); however, cultures on standard glass substantially detached before the analysis at later time points (>8 weeks). We observed similar soma size, neurite complexity (MAP2$^+$ dendrites) and presynaptic density (SYNAPSIN puncta) on the three surfaces at the earlier time point (4 weeks), and between glass-DAP and glass-AAM at the later time point (8 weeks) (Figures 6A–6D). Confirming the formation of mature synapses, we also observed similar colocalization of pre- and post-synaptic (PSD95) proteins on the 3 surfaces at the earlier time point (Figures S4F–S4H). These results demonstrate that DAP and AAM treatments support the formation of neurite arborization and synaptic circuits on glass for long periods, unlike standard glass.

Once synapses are formed, they require further maturation time to become active. We performed voltage-clamp whole-cell recordings of human hPSC neurons cultured on glass-DAP, glass-AAM, or standard glass to investigate excitatory and inhibitory synapse functionality after 5 and 21 weeks on each respective surface. α-Amino-3-hydroxy-5-methyl-4-isoxazolepropionic acid (AMPA)

(P) Highest AP peaks of neurons on glass-DAP (n = 15 + 17), glass-AAM (n = 13 + 20), and standard glass (n = 17) at 5 and 21 weeks, respectively. All data shown as means ± SEMs, p values calculated using Mann-Whitney tests, ns for p > 0.05.
(C)–(K) and (M)–(P) n replicates from 3–6 independent experiments per time point.

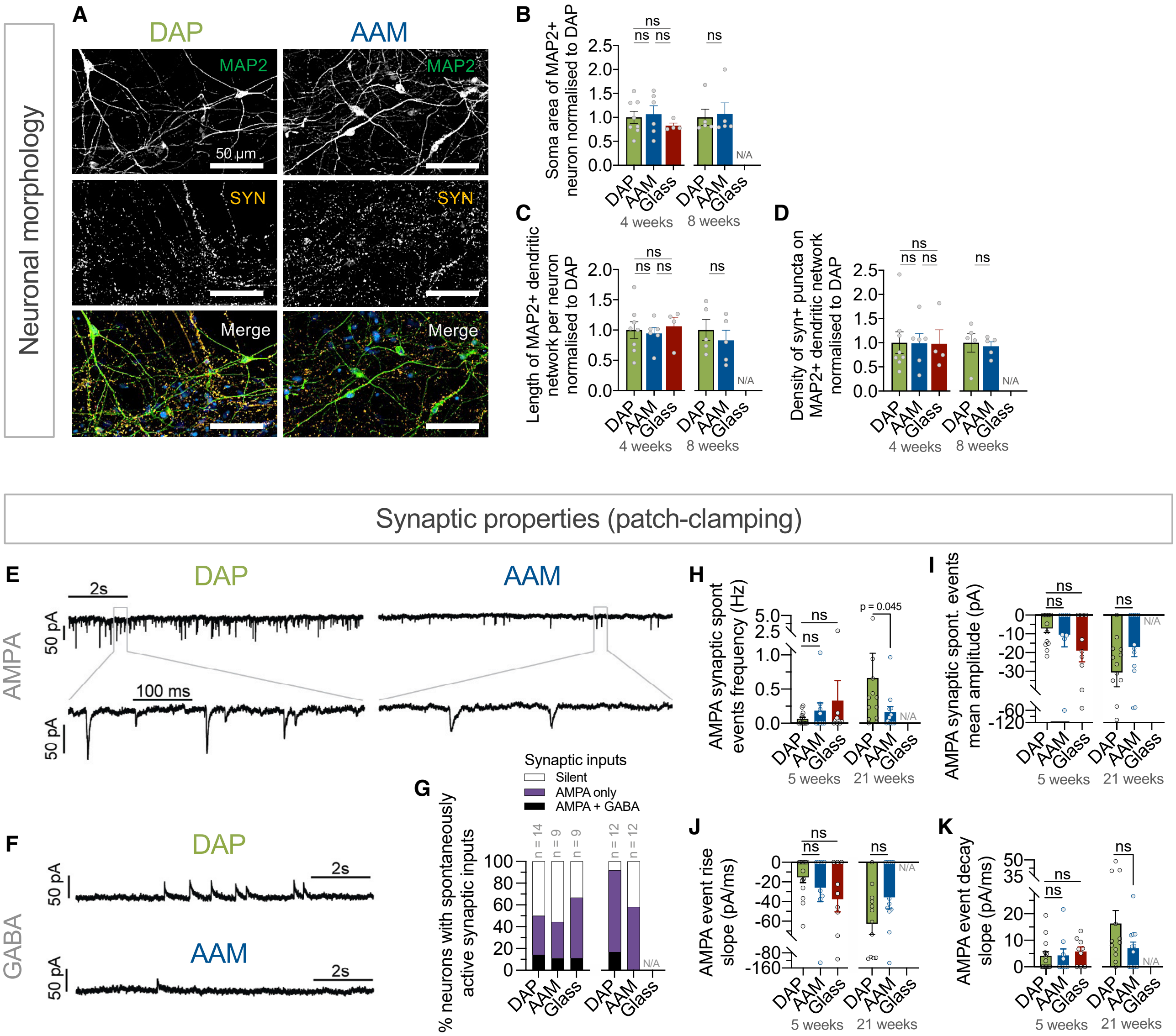

Figure 6. DAP-LAM surfaces promote the maturation of synaptically active neural networks

(A–D) Neurite and synapse morphology of cultures on glass-DAP, glass-AAM, and standard glass imaged using high-content confocal microscopy. Fold-change data normalized to glass-DAP for each time point, means ± SEMs shown (n = 4–8 replicates per surface per time point from 3 independent experiments). (A) Immunofluorescence staining of MAP2 and synapsin (SYN) in neuronal cultures on glass-DAP and glass-AAM after 9 weeks in maturation media. (B) Normalized fold change of soma area (mean of 70.8 μm^2 on glass-DAP). (C) Normalized fold change of total length of $MAP2^+$ dendritic network per neuron (mean of 583 μm per neuron on glass-DAP). (D) Normalized fold-change density of synapsin puncta per micron of $MAP2^+$ dendritic network (mean of 3 puncta per 10 μm on glass-DAP).

(E–K) Whole-cell patch clamp recordings of excitatory (glutamatergic AMPA receptor mediated) and inhibitory (GABAergic GABAa receptor mediated) events from midbrain neurons matured for 5 or 21 weeks on glass-DAP, glass-AAM, and standard glass pre-coated with PLO-Lam. (E and F) The traces represent spontaneous excitatory and inhibitory synaptic events recorded from functionally mature type 5 neurons on glass-DAP or glass-AAM at 21 weeks.

(G) Proportion of neurons (AP types 4 and 5 selected; n = 56) with spontaneously active synaptic inputs across 19 coverslips. Neurons with spontaneous excitatory or inhibitory synaptic events >0.01 Hz were considered active. (H–K) Spontaneous AMPA-mediated synaptic events frequency, mean amplitude, mean rise slope, and mean decay slope of each neuron (from total 19 coverslips). (B)–(D) and (G)–(K) Means ± SEMs shown; p values calculated using Mann-Whitney tests, ns for p > 0.05.

receptor-mediated events were recorded while the membrane potential was held artificially at −70 mV (reversal potential of anions; Figure 6E), and GABA receptor-mediated events at 0 mV (reversal potential of cation; Figure 6F). At the earlier time point (5 weeks), ∼50% of the neurons recorded on all of the surfaces received spontaneously active synaptic inputs either excitatory and/or inhibitory (Figure 6G). Despite some variance, the average kinetics and amplitude of AMPA synaptic events were comparable between surfaces (Figures 6I–6K). However, at the latest time point (21 weeks), neurons on standard glass detached substantially and were unusable. After 21 weeks in BrainPhys maturation medium, the proportion of synaptically active neurons increased to ∼90% on glass-DAP but remained ∼50% on glass-AAM (Figure 6G). Similarly, the frequency of spontaneous AMPA synaptic events was significantly higher on glass-DAP (Figure 6H), suggesting more functionally mature synapses. Overall, these results demonstrate that glass-DAP (coated with laminin) supports long-term maturation of active synaptic networks and outperforms glass-AAM and standard glass.

DAP-laminin surface supports live imaging and optogenetics applications in human neuronal cultures

Advanced electrophysiology methods are commonly combined with patch-clamping to further explore the biological principles underlying the circuitry and function of neuronal populations. As a proof of concept, to determine whether glass-DAP can be used for such applications, human neuronal cultures were prepared for either calcium imaging or optogenetics.

Assessing intracellular calcium changes via live imaging techniques provides insight into the electrical activity of hundreds of neurons simultaneously. Neuronal cultures on glass-DAP were transfected with Fluo-4-AM calcium dye and transferred into a perfusion chamber for live imaging. Calcium events were recorded over 4 min in BrainPhys Imaging medium (Zabolocki et al., 2020). Regions of interest were selected at the cell soma to monitor changes in intracellular Ca^{2+} over time (Figure 7A). Cells exhibiting calcium events with a $\Delta F/F_o$ >5% were determined to be spontaneously active. After 8 weeks of maturing on glass-DAP, we recorded a high proportion of active cells per field of view (64%) (Figures 7B and 7C). We observed spontaneous fast calcium spikes as well as slow calcium wave events (Figures 7D and 7E). The calcium events could be blocked by voltage-gated sodium channel antagonist application (tetrodotoxin [TTX]) (Figures 7C and 7E). These experiments demonstrate that glass-DAP supports live imaging applications of human neuronal populations, such as calcium imaging.

Optogenetic techniques modulate neuronal activity using light, allowing the precise exploration of functional neuronal circuitries. To determine whether glass-DAP could be used for optogenetics applications, we transfected human neuronal cultures with a lentivector to drive the expression of channelrhodopsin tagged with yellow fluorescent protein (ChETA-EYFP; Gunaydin et al., 2010) (Figure 7F). Blue light-emitting diode (LED) light (475 nm) was flashed for 5 ms at 100-ms intervals onto patch-clamped neurons using 0.1, 0.2, or 0.4 mW light intensities to evoke APs in BrainPhys Imaging medium (Figure 7G). Blue light stimulation of 0.4 mW evoked ∼500 pA of current, which was sufficient to trigger APs at an ∼100% success rate above a membrane potential of 10 mV (Figures 7H–7J). Spike-evoked success rates increased with light stimulation intensity (Figures 7G–7J). This was repeated to compare glass-DAP and glass-AAM, with no significant differences found between the surfaces (Figures S4I–S4L). Hence, glass-DAP supports applications requiring optogenetic control of human neuronal cultures.

DISCUSSION

Cell adhesion is determined by surface interactions between the cells and the cultureware. Surface modification of TCPS and glass cultureware is necessary to optimize these forces to ensure cell adhesion. hPSC-derived neuronal adhesion on standard glass is unreliable, hindering electrophysiology and imaging assays that require long-term cultures.

Physical properties of plasma polymers

Plasma polymerization can be used to modify cultureware surface chemistries without significantly affecting their macroscopic properties (Jacobs et al., 2012; Roach et al., 2007). The polymerization process deposits a highly stable (due to covalent bonding) randomly crosslinked thin plasma polymer film on the substrate (Michelmore et al., 2013, 2014; Ryssy et al., 2016). The physical properties of plasma polymer surfaces are highly tunable to the desired outcome, thereby benefiting many applications, including cell culture.

The resulting polymer surface physicochemistry depends on the properties of the gas entering the plasma reactor. In general, oxygen or air is used, increasing surface hydrophilicity and providing a negative surface charge. This process is used to generate TCPS from native polystyrene, which enables adequate adhesion for most cell types (Lerman et al., 2018). Specific monomers can be used to obtain the desired surface functionality (Jacobs et al., 2012). Amine-based monomers form amine-terminated plasma polymer surfaces characterized by a positive surface charge, which generally increases cell adhesion (due to attractive electrostatic interactions) and reduces

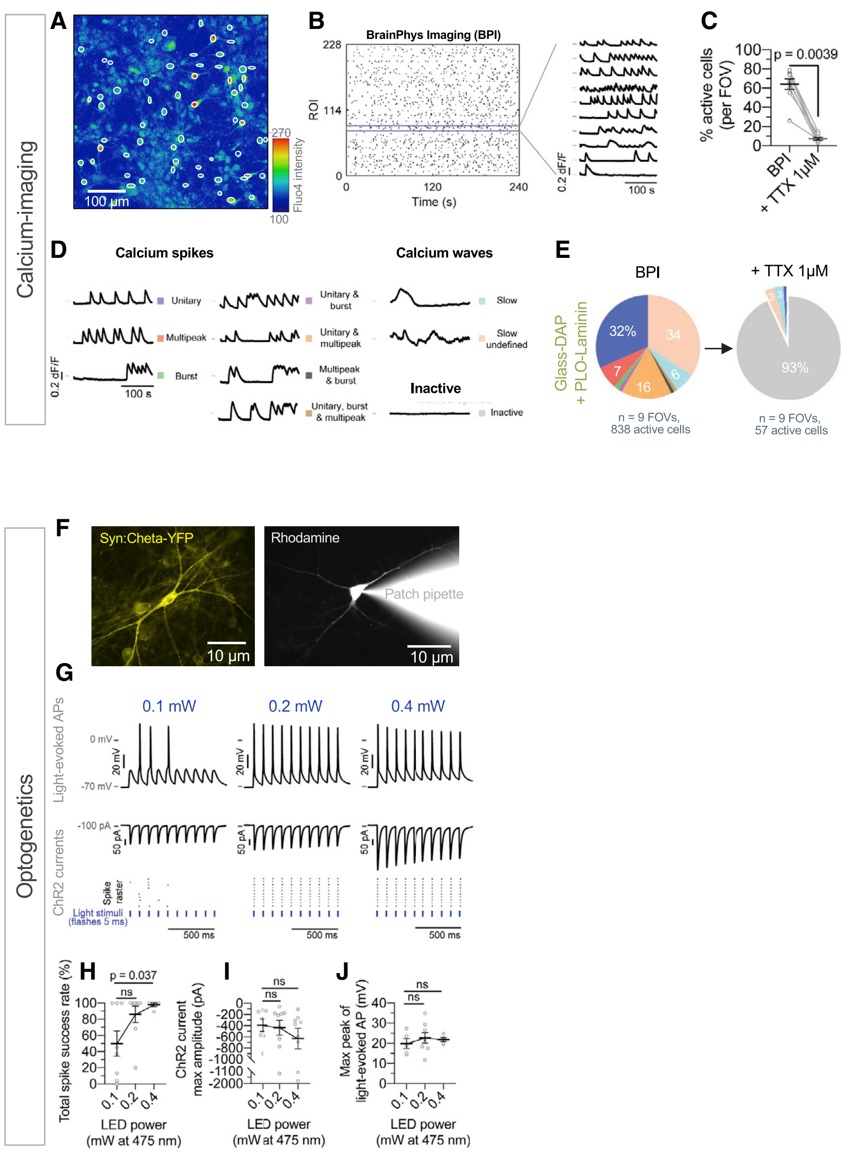

Figure 7. DAP-LAM-treated glass surfaces support calcium imaging and optogenetic applications in human neuronal models *in vitro*

(A–E) Calcium imaging recordings from hPSC-derived midbrain neurons after 10 weeks in maturation medium on glass-DAP with PLO-Lam. A total of 838 active regions of interest (ROIs) analyzed from 2 coverslips across 9 fields of view at the soma. (A) Example of an “active” neuronal population following Fluo-4-AM calcium dye incubation. White circles represent analyzed ROIs. (B) Example raster plots and calcium traces of active neurons showing spontaneous calcium events recorded over 4 min on glass-DAP in BrainPhys Imaging. (C) Mean % of active cells on glass-DAP with or without tetrodotoxin (TTX). Cells considered active if $\Delta F/F_0 > 5\%$ from baseline. (D) Example traces of calcium events categorized into spontaneous calcium spikes (fast rising phase) and calcium waves (slow rising phases). (E) Proportion of active cells and their event types on glass-DAP following TTX perfusion.

(F–J) Optogenetic responses of neurons on glass-DAP. Mature neurons (type 5, n = 9 across 4 coverslips) were patch-clamped and subject to 10 × 5 ms flashes of blue (475 nm) LED light of various intensities. (F) Example images of live neurons expressing the optogene synapsin:ChETA-YFP (left) and filled with rhodamine (right). (G) Typical optogenetic responses from the same patch-clamped neuron to blue LED stimuli at 0.1, 0.2, and 0.4 mW of power. Top: APs evoked by channelrhodopsin 2 (ChR2) membrane depolarization in current-clamp. Bottom: ChR2-mediated currents in voltage-clamp, held at −70 mV (H) Total spike success rate (%) of each neuron across 10 sweeps. Spikes >−10 mV in amplitude were included. (I and J) Maximum amplitudes of ChR2-mediated currents (I) and (J) of APs evoked by ChR2-mediated membrane depolarization.

(B) and (H)–(J) Means ± SEMs. (B) p values calculated with 2-tailed paired Wilcoxon and (H)–(J) 2-tailed parametric unpaired tests, ns for p > 0.05.

cell clustering (Dadsetan et al., 2009; Kirby et al., 2017; Palyvoda et al., 2008). While other systems introducing positive charge (mostly via nitrogen-containing surface functional groups) have been successful for multiple cell types (Granato et al., 2018; Lee et al., 2017; Lee and Schmidt, 2015; Meade et al., 2013), plasma polymer surfaces were only demonstrated to improve adhesion for human fibroblasts (Hamerli, 2003; Jacobs et al., 2012; Štrbková et al., 2016) and rarely studied for neurons (Harsch et al., 2000) or other cells (Smith et al., 2016). Other glass surface modifications for neuron cultures have focused on neurite outgrowth (Cesca et al., 2014; Corey et al., 1991; Li et al., 2015; Liu et al., 2006) or neural stem cell differentiation (Ananthanarayanan et al., 2010; Chen et al., 2018b), but not sustained neuronal adhesion. Recently nano-structured glass was shown to facilitate PSC-derived neuron functionality (Harberts et al., 2021), but again, cultures were not tested >20 days. An additional benefit of plasma polymer treatment is that the refractive index (and hence, magnitude of attractive van der Waals interactions) can be tailored to further promote the adhesion of various cell types. Here, we tested plasma polymer films with the specific intent to increase adhesion for neuronal cultures.

Supporting cell adhesion with plasma polymer films requires a balance between surface charge and surface energy. We show the amine-based DAP plasma polymer treatment generates a positively charged, hydrophilic surface with the greatest neuronal adhesion-promoting ability of all of the tested polymer treatments.

The DAP monomer is known to be a by-product of plant metabolism in response to osmotic stress. Polyamines involved in plant stress tolerance are oxidized to DAP under stress conditions, in which DAP acts as a precursor in osmoprotective arginine/proline and β-alanine metabolic pathways. This response is present in crop plants (Pal et al., 2018; Parthasarathy et al., 2019) and flowering plants (Duhazé et al., 2002; Jammes et al., 2014). DAP has also been shown to modulate membrane electrical and ion transport properties in plants to facilitate stomatal closing during stress (Jammes et al., 2014). However, to our knowledge, this is the first time that DAP has been identified as a useful surface treatment for cell adhesion *in vitro*.

We identified AAM as another amine-terminated, positively charged plasma polymer treatment that supports sustained neuronal adhesion. However, glass-AAM was less positively charged and displayed slightly inferior properties, including less support for functional synapses compared to glass-DAP. The DAP monomer had a greater number of nitrogen-containing functional groups than the AAM monomer, resulting in a higher density of amine surface groups in the plasma polymer film (Ryssy et al., 2016; Smith et al., 2016). Moreover, the attractive van der Waals interactions are stronger between cells and glass-DAP than between cells and glass-AAM, as the refractive index of DAP is higher than that of AAM. Therefore, glass-DAP, having the highest positive surface charge (strongest attractive electrostatic double-layer forces) and the highest refractive index (strongest attractive van der Waals interactions) of all of the modified surfaces tested, best supports sustained neuronal adhesion and neurophysiological function in combination with the relevant ECM.

Interaction between plasma polymerized films and polymeric/ECM coatings

Conventional cell culture on standard glass and TCPS uses a combination of polymeric/ECM coatings to provide the required surface conditions for cell adhesion. On both glass and TCPS, adhesion is highly variable (Smith et al., 2016; Yamamoto et al., 1998, 2000), but it is temporarily stabilized with polymeric/ECM coatings. Optimal neuronal adhesion is 2-fold. First, polymeric attachment factors such as PLO and polylysine (PLL) are added to provide a positive surface charge that is most favorable for neuronal adhesion (Anselme et al., 2010; Kirby et al., 2017; Palyvoda et al., 2008). The positive charge, consequent to a dissociation of surface amine groups, results in attractive electric double-layer interactions between the polymer surface and the negatively charged cell membrane (Chen et al., 2018a; Stenger et al., 1993). Second, ECM proteins are added to provide adequate surface topography (Anselme et al., 2010; Palyvoda et al., 2008). Laminin and Matrigel (a mixture of collagen and laminin) are found abundantly in the natural ECM and are commonly used *in vitro* to provide a topographic framework favorable for adhesion (Anselme et al., 2010). PLO coating with additional laminin for at least 24 h (PLO-Lam) is often considered the most favorable for human neuronal adhesion. However, no combination of polymeric/ECM coatings was previously evaluated for long-term neuronal cultures on standard glass. Here, we show that PLO-Lam on glass-DAP sustained neuronal adhesion for considerably longer than standard glass with any tested polymeric/ECM coating, highlighting DAP as a critical surface modification. We also show that the combinations DAP-LAM and DAP-Matrigel performed comparably to DAP-PLO-Lam. Given that DAP already provides the ideal physicochemical environment, we speculate that this renders the PLO function redundant, hence the similar performance in Matrigel and laminin conditions. This redundancy occurs due to PLO and DAP's providing similar surface chemistry (Harnett et al., 2007); however, they differ in their chemical bond to the substrate. The plasma polymerization process to generate DAP results in a highly crosslinked film covalently bound to the substrate (Jacobs et al., 2012; Michelmore et al., 2016; Rao and Winter, 2009). Consequently, DAP is highly stable and resistant to degradation (Daunton et al., 2015; Michelmore et al., 2016). In contrast, polymeric coatings such as PLO, which are deposited from a solution, are weakly bound to the substrate (Rao and Winter, 2009) and therefore easier to degrade in culture. Plasma polymer deposition for desired surface chemistry is more reliable than solution-based methods, whereby DAP is most suitable for neuronal cultures. Plasma polymerization creates an ultrathin layer (33 nm for DAP) that does not modify the surface topography (Michelmore et al., 2016; Nguyen et al., 2016). However, additional laminin-based ECM coatings may increase surface roughness (Jain et al., 2020) and promote integrin-mediated cell adhesion (De Arcangelis and Georges-Labouesse, 2000) to further sustain long-term adherence.

While we have shown that long-term neuronal adhesion on glass is optimal on glass-DAP-PLO-Lam, this remains unchanged with no extra PLO coating. Long-term adhesion is supported optimally on glass-DAP-LAM as is neuronal functionality (Figures S4B). Based on this, PLO becomes unnecessary when using DAP-coated surfaces.

Brain-specific cell types supported by glass-DAP

We discovered that DAP plasma polymer treatment on glass addresses limitations in long-term human neuronal culture adhesion. We show that glass-DAP-LAM surfaces support long-term adhesion, differentiation, and maturation of hPSC-derived midbrain and cortical neurons and astrocytes. While we cannot test all neuronal types, no experiment that we performed indicated that the DAP surface preferentially supports a particular brain cell type. Cells along the glial and neuronal lineage such as GBMs, GPCs, and NPCs perform favorably on glass-DAP-Matrigel surfaces. We found comparable improved adhesion with different cell-plating methods such as replating post-mitotic neurons or direct NPC differentiation on surfaces (Figures S1A–S1D). In contrast, pluripotent stem cells still prefer a TCPS substrate and may require a polymer with different properties; however, glass-DAP-Matrigel surfaces support stem cell colonies better than standard glass with Matrigel. Rodent primary neurons mature significantly faster than human neurons and do not usually require long-term adhesion. Therefore, the study focused on human brain cells, and further experimentation will be required to demonstrate the potential benefits of DAP coating for non-human cells.

Applications of glass-DAP coverslips

Patient-derived iPSCs are increasingly popular pre-clinical models of neurological and psychiatric disorders (Bardy et al., 2020; Chailangkarn et al., 2016; Israel et al., 2012; Mertens et al., 2016; Sarkar et al., 2018; Tran et al., 2020; van den Hurk and Bardy, 2019). Two-dimensional monolayer models offer reproducible and relatively high-throughput drug screening capabilities. However, variability exists within these models, despite the use of standard cell culture protocols and cultureware (Volpato and Webber, 2020). Standard polymeric adhesive factors (e.g., PLO, PLL) for culture degrade over extended culture times and increase variability. Plasma polymerized DAP surfaces are consistently uniform and highly stable (Gengenbach and Griesser, 1999; Jacobs et al., 2012; Michelmore et al., 2016), and reduce experimental variability and increase statistical power. Plasma polymerization is highly reproducible, with a relatively low cost and environmental burden (Iqbal et al., 2019; Jang et al., 2021), so it can be easily upscaled for research such as drug discovery. We expect that DAP plasma polymer is unlikely to interfere with experimental substances in such assays despite its positive charge given the high stability of DAP and the current use of solution-based positive charge layers added in standard drug discovery assays (Darville et al., 2016; Ryan et al., 2013, 2016), where interference is not reported. Plasma polymerization allows DAP to be deposited on objects of complex geometries, thus also providing potential future applications for 3D neuronal culture.

Electrophysiology, including patch-clamping and live functional imaging, is the gold standard method to study neuronal function. While TCPS may sufficiently promote neuronal adhesion, its application in electrophysiology and imaging is limited. Transferable glass coverslips are preferred for patch-clamping and live imaging assays because their weight provides a more stable anchor than lighter plastic material; therefore, microscopic movements are minimized during recordings. TCPS also scatters light more than glass, which reduces imaging quality (Lerman et al., 2018). DAP-treated glass coverslips or plates will therefore be ideal for virtually all imaging assays (live or fixed) requiring high optical resolution, such as highly magnified synapses or organelles, for example. Finally, plasma polymerization of DAP can also be applied to TCPS if plastic is preferred (Figures S1E–S1J), perhaps for practical or economic reasons. Applying DAP plasma polymer to multi-electrode array plates requires further investigation. Plasma polymerization would need to be performed without insulating the electrodes. In addition, the material used on the culture surface of a multielectrode array (MEA) plate is generally unknown (proprietary). However, MEA plates using TCPS may not benefit from DAP coating as much as glass would.

Conclusions

DAP-LAM-treated cultureware provides the optimal microenvironment for long-term neuronal adhesion and functional maturation, benefiting models of human brain diseases often confounded by cell detachment over extended periods. Plasma polymerization deposits strongly onto virtually any substrate (Aziz et al., 2015, 2018) and on objects of complex geometries (Michelmore et al., 2016). Therefore, the DAP treatment can be applied to various cultureware to maintain specific cell surface properties and experimental homogeneity. DAP-treated cultureware with laminin-based coating provides a reproducible and stable microenvironment that extends adhesion of a range of human brain cells (mature neurons, astrocytes, and proliferating neural/glia cells). The novel application of DAP as a surface modification for neuronal adhesion is timely given the rapid expansion of innovative pre-clinical patient-derived neuronal models and electrophysiological and imaging assays. DAP surface treatment will improve the quality of *in vitro* human neuronal models, and therefore will facilitate translation in neurology and psychiatry.

EXPERIMENTAL PROCEDURES

A detailed description of the Experimental procedures is provided in the supplemental information.

Plasma polymerization

Plasma polymerization was performed using a custom-built plasma reactor, as described previously as comprising a cylindrical stainless steel vacuum vessel (diameter 30 cm, volume 20 L) (Michelmore et al., 2013; Smith et al., 2016). Plasma parameters were optimized for maximum functional group retention (Table S1).

Maturation of neural progenitors to neurons and plating on test surfaces

For neuronal maturation, hESC neural progenitors were seeded at 7.9×10^4–2.10×10^5 cells/cm^2 in neural progenitor medium (NPM) (see Supplemental experimental procedures) on TCPS or glass coverslips. The next day, neuronal maturation media (NMM) was added (BrainPhys Neuronal Medium [Bardy et al., 2015; cat. no. 05790, STEMCELL Technologies] with supplements [see Supplemental experimental procedures]). For most of the experiments, NPCs were differentiated into post-mitotic neuronal cultures for 2 weeks in NMM, then live cell (DAPI) sorted (BD FACSMelody) and replated at 1.58×10^5–2.1×10^5 cells/cm^2 on TCPS, coated glass coverslips, or standard glass coverslips, in NMM containing half-concentrations of growth factors (Figures 1, 2, and 3, detachment; Figure 6, morphology; and Figures 5, 6, and 7, electrophysiology). In a few experiments, neuron cultures were cultivated directly onto test surfaces without the fluorescence-activated cell sorting (FACS) sorting step (Figure 4, FACS viability; Figures 1, 2, and 3, detachment). The same protocol was used in each experiment comparing the effect of the substrates. All of the periods stated correspond to the time that neuronal cultures spent on the test surface only (Figure S1).

Quantification of cell detachment

Neuronal cultures were imaged at 4× magnification in phase contrast (CoolLED PE4000) on an inverted microscope (Olympus IX73) biweekly for the duration of the experiments. ImageJ software (Schneider et al., 2012) was used to define the detached regions and calculate the total detached surface area.

Immunostaining and image analysis

Cells were fixed for 10 min in 4% paraformaldehyde at room temperature (RT) and treated with 0.1% Triton X-100 with 3% donkey serum in 0.1 M Tris-buffered saline for 60 min. Cells were incubated with primary antibodies against Synapsin-I (1:500; cat. no. AB1543P, Merck), GFAP (1:200; cat. no. ab4648, Abcam), MAP2 (1:2000; cat. no. ab5392, Abcam), and PSD95 (1:500; cat. no. ab13552, Abcam) at 4°C overnight, and then incubated with fluorescence-tagged secondary antibodies (1:250; Abcam) at RT for 60 min. After incubation, coverslips were stained with 4′,6-diamidino-2-phenylindole (DAPI; cat. no. D9542, Sigma) before mounting and sealing.

Whole-cell patch-clamp recordings

Human neurons cultured on DAP, AAM, or glass coverslips were transferred into a recording chamber and perfused with artificial cerebrospinal fluid (ACSF) or BrainPhys Imaging (cat. no. 05796, STEMCELL Technologies; Zabolocki et al., 2020) at RT (21°C–23°C). Following successful seal formation (>1GΩ) and break-in, cells received a −5-mV test pulse in voltage-clamp to determine access resistance, membrane resistance, and capacitance. To record voltage-gated sodium (Nav) and potassium (Kv) channel currents, cells were patch-clamped, held at −70 mV in voltage-clamp, and injected with incremental current steps (+5 or +10 mV) across 15 sweeps following an initial decrease to −75 mV. Amplitudes of slow-inactivating and rapidly inactivating Kv currents were measured, respectively, at −10 mV membrane potentials and maximum Nav currents. Resting membrane potentials were recorded in current-clamp and held with 0 pA of current, following evoked AP recordings. AMPA receptor-mediated events were observed in voltage-clamp at −70 mV (close to Cl^- reversal potential) and in GABAa-receptor events in voltage-clamp at 0 mV (close to Na^+ reversal potential). Total AMPA or GABAa patch-recording lengths were up to 180 s, conducted in a gap-free run. AMPA and GABA events with an event duration of 1–10 or 10–100 ms, respectively, were included for further analysis. AMPA synaptic events were fitted with a 6-terms sum of exponentials to determine their kinetics and amplitudes.

Analysis and statistics

We were blinded to all of the plasma polymer-treated surfaces tested. Unblinding occurred only after cell phenotypic analyses were performed. For each independent experiment, the same cell batch and cultureware were used and different substrates were tested side by side to reduce the technical variability bias. All of the treated glass surfaces were prepared at the same time within each experiment. Statistical analysis was performed using Prism 9. Normality was not assumed for samples with <50 replicates. Statistical significance was assessed using two-tailed non-parametric unpaired (Mann-Whitney) or two-tailed paired Wilcoxon tests.

Data and code availability

The raw data are freely available upon reasonable request to the corresponding author. DAP-coated coverslips can be made available upon reasonable request to the corresponding author.

SUPPLEMENTAL INFORMATION

Supplemental information can be found online at https://doi.org/10.1016/j.stemcr.2022.01.013.

AUTHOR CONTRIBUTIONS

Conceptualization, C.B., T.S., and J.D.W.; methodology, C.B., T.S., and B.M; investigation, B.M., S.A.A.-B., L.E.S., M.K., M.v.d.H., M.Z., A.W., P.M., R.A., L.T., I.I., B.W.S., and Z.G.; writing, C.B. and B.M., with feedback from all of the authors; resources, R.O. and S.P., funding acquisition, C.B. and T.S.

CONFLICTS OF INTEREST

The authors declare no competing interests.

ACKNOWLEDGMENTS

This work was generously supported by Perpetual Impact Philanthropy, the Brain Foundation, the Rebecca L. Cooper foundation, Australia, the Ian Potter Foundation, Michael and Angelique Boileau Corporate Philanthropy, The Hospital Research Foundation: Parkinson's South Australia, The Michael J Fox Foundation, The Shake It Up Foundation Australia, The Grosset Gaia Foundation, The Mark Hugues Foundation, Cancer Council SA, Cancer Australia, Cooperative Research Centre for Cell Therapy Manufacturing, Australia, and the MRFF Australian Government and Department of Health, Australian Research Council LIEF grant (to C.B.); the Netherlands Organisation for Scientific Research Rubicon Fellowship 019.163LW.032 (to M.v.d.H.); the Flinders University Research Scholarship (to M.Z. and B.M.); and the Australian Government Research Training Program Scholarship (to R.A.). Flow cytometry analysis and cell sorting were performed at the South Australian Health Medical Research Institute (SAHMRI) in the ACRF Cellular Imaging and Cytometry Core Facility. The facility is generously supported by the Detmold Hoopman Group, the Australian Cancer Research Foundation, and the Australian government through the Zero Childhood Cancer Program.

Received: July 2, 2021
Revised: January 16, 2022
Accepted: January 17, 2022
Published: February 17, 2022

REFERENCES

Ananthanarayanan, B., Little, L., Schaffer, D.V., Healy, K.E., and Tirrell, M. (2010). Neural stem cell adhesion and proliferation on phospholipid bilayers functionalized with RGD peptides. Biomaterials *31*, 8706–8715.

Anselme, K., Ploux, L., and Ponche, A. (2010). Cell/material interfaces: influence of surface chemistry and surface topography on cell adhesion. J. Adhes. Sci. Technol. *24*, 831–852.

Aziz, G., De Geyter, N., and Morent, R. (2015). Incorporation of primary amines via plasma technology on biomaterials. Advances in Bioengineering, pp. 21–48. https://doi.org/10.5772/59691.

Aziz, G., Ghobeira, R., Morent, R., and De Geyter, N. (2018). Plasma polymerization for tissue engineering purposes. Recent Research in Polymerization, *69*.

Bardy, C., Greenberg, Z., Perry, S.W., and Licinio, J. (2020). Chapter 12 - personalized psychiatry with human iPSCs and neuronal reprogramming. In Personalized Psychiatry, B.T. Baune, ed. (San Diego: Academic Press), pp. 127–146.

Bardy, C., van den Hurk, M., Eames, T., Marchand, C., Hernandez, R.K., Gorris, M., Galet, B., Palomares, V., Brown, J., Bang, A., et al. (2015). Neuronal medium that supports basic synaptic functions and activity of human neurons in vitro. Proc. Natl. Acad. Sci. U S A. *112*, E3312.

Bardy, C., van den Hurk, M., Kakaradov, B., Erwin, J.A., Jaeger, B.N., Hernandez, R.V., Eames, T., Paucar, A.A., Gorris, M., Marchand, C., et al. (2016). Predicting the functional states of human iPSC-derived neurons with single-cell RNA-seq and electrophysiology. Mol. Psychiatry *21*, 1573–1588.

Cesca, F., Limongi, T., Accardo, A., Rocchi, A., Orlando, M., Shalabaeva, V., Di Fabrizio, E., and Benfenati, F. (2014). Fabrication of biocompatible free-standing nanopatterned films for primary neuronal cultures. RSC Adv. *4*, 45696–45702.

Chailangkarn, T., Trujillo, C.A., Freitas, B.C., Hrvoj-Mihic, B., Herai, R.H., Yu, D.X., Brown, T.T., Marchetto, M.C., Bardy, C., McHenry, L., et al. (2016). A human neurodevelopmental model for Williams syndrome. Nature *536*, 338–343.

Chen, L., Yan, C., and Zheng, Z. (2018a). Functional polymer surfaces for controlling cell behaviors. Mater. Today *21*, 38–59.

Chen, W., Han, S., Qian, W., Weng, S., Yang, H., Sun, Y., Villa-Diaz, L.G., Krebsbach, P.H., and Fu, J. (2018b). Nanotopography regulates motor neuron differentiation of human pluripotent stem cells. Nanoscale *10*, 3556–3565.

Corey, J.M., Wheeler, B.C., and Brewer, G.J. (1991). Compliance of hippocampal neurons to patterned substrate networks. J. Neurosci. Res. *30*, 300–307.

Dadsetan, M., Knight, A.M., Lu, L., Windebank, A.J., and Yaszemski, M.J. (2009). Stimulation of neurite outgrowth using positively charged hydrogels. Biomaterials *30*, 3874–3881.

Darville, H., Poulet, A., Rodet-Amsellem, F., Chatrousse, L., Pernelle, J., Boissart, C., Héron, D., Nava, C., Perrier, A., Jarrige, M., et al. (2016). Human pluripotent stem cell-derived cortical neurons for high throughput medication screening in autism: a proof of concept study in SHANK3 haploinsufficiency syndrome. EBioMedicine *9*, 293–305.

Daunton, C., Smith, L.E., Whittle, J.D., Short, R.D., Steele, D.A., and Michelmore, A. (2015). Plasma parameter aspects in the fabrication of stable Amine functionalized plasma polymer films. Plasma Process. Polym. *12*, 817–826.

De Arcangelis, A., and Georges-Labouesse, E. (2000). Integrin and ECM functions: roles in vertebrate development. Trends Genet. *16*, 389–395.

Di Lullo, E., and Kriegstein, A.R. (2017). The use of brain organoids to investigate neural development and disease. Nat. Rev. Neurosci. *18*, 573–584.

Duhazé, C., Gouzerh, G., Gagneul, D., Larher, F., and Bouchereau, A. (2002). The conversion of spermidine to putrescine and 1,3-diaminopropane in the roots of Limonium tataricum. Plant Sci. *163*, 639–646.

Duval, K., Grover, H., Han, L.H., Mou, Y., Pegoraro, A.F., Fredberg, J., and Chen, Z. (2017). Modeling physiological events in 2D vs. 3D cell culture. Physiology (Bethesda) *32*, 266–277.

Ebert, A.D., Liang, P., and Wu, J.C. (2012). Induced pluripotent stem cells as a disease modeling and drug screening platform. J. Cardiovasc. Pharmacol. *60*, 408–416.

Gengenbach, T.R., and Griesser, H.J. (1999). Aging of 1,3-diaminopropane plasma-deposited polymer films: mechanisms and reaction pathways. J. Polym. Sci. A Polym. Chem. *37*, 2191–2206.

Gomez, N., Lu, Y., Chen, S., and Schmidt, C.E. (2007). Immobilized nerve growth factor and microtopography have distinct effects on polarization versus axon elongation in hippocampal cells in culture. Biomaterials *28*, 271–284.

Gomez, N., and Schmidt, C.E. (2007). Nerve growth factor-immobilized polypyrrole: bioactive electrically conducting polymer for enhanced neurite extension. J. Biomed. Mater. Res. A. *81*, 135–149.

Granato, A.E.C., Ribeiro, A.C., Marciano, F.R., Rodrigues, B.V.M., Lobo, A.O., and Porcionatto, M. (2018). Polypyrrole increases branching and neurite extension by Neuro2A cells on PBAT ultrathin fibers. Nanomedicine *14*, 1753–1763.

Gunaydin, L.A., Yizhar, O., Berndt, A., Sohal, V.S., Deisseroth, K., and Hegemann, P. (2010). Ultrafast optogenetic control. Nat. Neurosci. *13*, 387–392.

Hamazaki, T., El Rouby, N., Fredette, N.C., Santostefano, K.E., and Terada, N. (2017). Concise review: induced pluripotent stem cell research in the era of precision medicine. Stem Cells *35*, 545–550.

Hamerli, P. (2003). Surface properties of and cell adhesion onto allylamine-plasma-coated polyethylenterephtalat membranes. Biomaterials *24*, 3989–3999.

Harberts, J., Siegmund, M., Schnelle, M., Zhang, T., Lei, Y., Yu, L., Zierold, R., and Blick, R.H. (2021). Robust neuronal differentiation of human iPSC-derived neural progenitor cells cultured on densely-spaced spiky silicon nanowire arrays. Scientific Rep. *11*, 18819.

Harnett, E.M., Alderman, J., and Wood, T. (2007). The surface energy of various biomaterials coated with adhesion molecules used in cell culture. Colloids Surf. B Biointerfaces *55*, 90–97.

Harsch, A., Calderon, J., Timmons, R.B., and Gross, G.W. (2000). Pulsed plasma deposition of allylamine on polysiloxane: a stable surface for neuronal cell adhesion. J. Neurosci. Methods *98*, 135–144.

Iqbal, M., Dinh, D.K., Abbas, Q., Imran, M., Sattar, H., and Ul Ahmad, A. (2019). Controlled Surface Wettability by Plasma Polymer Surface Modification, *2* (Surfaces), p. 26.

Israel, M.A., Yuan, S.H., Bardy, C., Reyna, S.M., Mu, Y., Herrera, C., Hefferan, M.P., Van Gorp, S., Nazor, K.L., Boscolo, F.S., et al. (2012). Probing sporadic and familial Alzheimer's disease using induced pluripotent stem cells. Nature *482*, 216–220.

Jacobs, T., Morent, R., De Geyter, N., Dubruel, P., and Leys, C. (2012). Plasma surface modification of biomedical polymers: influence on cell-material interaction. Plasma Chem. Plasma Process. *32*, 1039–1073.

Jain, D., Mattiassi, S., Goh, E.L., and Yim, E.K.F. (2020). Extracellular matrix and biomimetic engineering microenvironment for neuronal differentiation. Neural Regen. Res. *15*, 573–585.

Jammes, F., Leonhardt, N., Tran, D., Bousserouel, H., Very, A.A., Renou, J.P., Vavasseur, A., Kwak, J.M., Sentenac, H., Bouteau, F., et al. (2014). Acetylated 1,3-diaminopropane antagonizes abscisic acid-mediated stomatal closing in Arabidopsis. Plant J. *79*, 322–333.

Jang, H.J., Jung, E.Y., Parsons, T., Tae, H.-S., and Park, C.-S. (2021). A review of plasma synthesis methods for polymer films and nanoparticles under atmospheric pressure conditions. Polymers *13*, 2267.

Kim, J., Koo, B.K., and Knoblich, J.A. (2020). Human organoids: model systems for human biology and medicine. Nat. Rev. Mol. Cell Biol. *21*, 571–584.

Kirby, G.T., Mills, S.J., Vandenpoel, L., Pinxteren, J., Ting, A., Short, R.D., Cowin, A.J., Michelmore, A., and Smith, L.E. (2017). Development of advanced dressings for the delivery of progenitor cells. ACS Appl. Mater. Inter. *9*, 3445–3454.

Lakard, S., Herlem, G., Propper, A., Kastner, A., Michel, G., Valles-Villarreal, N., Gharbi, T., and Fahys, B. (2004). Adhesion and proliferation of cells on new polymers modified biomaterials. Bioelectrochemistry *62*, 19–27.

Lancaster, M.A., Renner, M., Martin, C.A., Wenzel, D., Bicknell, L.S., Hurles, M.E., Homfray, T., Penninger, J.M., Jackson, A.P., and Knoblich, J.A. (2013). Cerebral organoids model human brain development and microcephaly. Nature *501*, 373–379.

Lee, C., Kim, S.H., Jang, J.H., and Lee, S.Y. (2017). Enhanced cell adhesion on a nano-embossed, sticky surface prepared by the printing of a DOPA-bolaamphiphile assembly ink. Sci. Rep. *7*, 13797.

Lee, J.Y., and Schmidt, C.E. (2015). Amine-functionalized polypyrrole: inherently cell adhesive conducting polymer. J. Biomed. Mater. Res. A. *103*, 2126–2132.

Leipzig, N.D., Xu, C., Zahir, T., and Shoichet, M.S. (2009). Functional immobilization of interferon-gamma induces neuronal differentiation of neural stem cells. J. Biomed. Mater. Res. A *93*, 625–633.

Lerman, M.J., Lembong, J., Muramoto, S., Gillen, G., and Fisher, J.P. (2018). The evolution of polystyrene as a cell culture. Mater. Tissue Eng. B: Rev. *24*, 359–372.

Li, P., Greben, K., Wördenweber, R., Simon, U., Offenhäusser, A., and Mayer, D. (2015). Tuning neuron adhesion and neurite guiding using functionalized AuNPs and backfill chemistry. RSC Adv. *5*, 39252–39262.

Liu, B.F., Ma, J., Xu, Q.Y., and Cui, F.Z. (2006). Regulation of charged groups and laminin patterns for selective neuronal adhesion. Colloids Surf. B: Biointerfaces *53*, 175–178.

Liu, C., Oikonomopoulos, A., Sayed, N., and Wu, J.C. (2018). Modeling human diseases with induced pluripotent stem cells: from 2D to 3D and beyond. Developmentl *145*, dev156166.

Meade, K.A., White, K.J., Pickford, C.E., Holley, R.J., Marson, A., Tillotson, D., van Kuppevelt, T.H., Whittle, J.D., Day, A.J., and Merry, C.L. (2013). Immobilization of heparan sulfate on electrospun meshes to support embryonic stem cell culture and differentiation. J. Biol. Chem. *288*, 5530–5538.

Mertens, J., Marchetto, M.C., Bardy, C., and Gage, F.H. (2016). Evaluating cell reprogramming, differentiation and conversion technologies in neuroscience. Nat. Rev. Neurosci. *17*, 424–437.

Michelmore, A., Steele, D.A., Robinson, D.E., Whittle, J.D., and Short, R.D. (2013). The link between mechanisms of deposition and the physico-chemical properties of plasma polymer films. Soft Matter. *9*, 6167–6175.

Michelmore, A., Whittle, J.D., Bradley, J.W., and Short, R.D. (2016). Where physics meets chemistry: thin film deposition from reactive plasmas. Front. Chem. Sci. Eng. *10*, 441–458.

Michelmore, A., Whittle, J.D., Short, R.D., Boswell, R.W., and Charles, C. (2014). An experimental and analytical study of an asymmetric capacitively coupled plasma used for plasma polymerization. Plasma Process. Polym. *11*, 833–841.

Mouw, J.K., Ou, G., and Weaver, V.M. (2014). Extracellular matrix assembly: a multiscale deconstruction. Nat. Rev. Mol. Cell Biol *15*, 771–785.

Nguyen, A.T., Sathe, S.R., and Yim, E.K.F. (2016). From nano to micro: topographical scale and its impact on cell adhesion, morphology and contact guidance. J. Phys. Condensed Matter *28*, 183001.

Nirwane, A., and Yao, Y. (2018). Laminins and their receptors in the CNS. Biol. Rev. Camb Philos. Soc. https://doi.org/10.1111/brv.12454.

Pal, M., Tajti, J., Szalai, G., Peeva, V., Vegh, B., and Janda, T. (2018). Interaction of polyamines, abscisic acid and proline under osmotic stress in the leaves of wheat plants. Sci. Rep. *8*, 12839.

Palyvoda, O., Bordenyuk, A.N., Yatawara, A.K., McCullen, E., Chen, C., Benderskii, A.V., and Auner, G.W. (2008). Molecular organization in SAMs used for neuronal cell growth. Langmuir *24*, 4097–4106.

Parr, C.J.C., Yamanaka, S., and Saito, H. (2017). An update on stem cell biology and engineering for brain development. Mol. Psychiatry *22*, 808–819.

Parthasarathy, A., Savka, M.A., and Hudson, A.O. (2019). The synthesis and role of beta-alanine in plants. Front. Plant Sci. *10*, 921.

Rao, S.S., and Winter, J.O. (2009). Adhesion molecule-modified biomaterials for neural tissue engineering. Front. Neuroeng *2*, 6.

Ray, B., Chopra, N., Long, J.M., and Lahiri, D.K. (2014). Human primary mixed brain cultures: preparation, differentiation, characterization and application to neuroscience research. Mol. Brain *7*, 63.

Roach, P., Eglin, D., Rohde, K., and Perry, C.C. (2007). Modern biomaterials: a review - bulk properties and implications of surface modifications. J. Mater. Sci. Mater. Med. *18*, 1263–1277.

Rowe, R.G., and Daley, G.Q. (2019). Induced pluripotent stem cells in disease modelling and drug discovery. Nat. Rev. Genet. *20*, 377–388.

Ryan, K.R., Sirenko, O., Parham, F., Hsieh, J.-H., Cromwell, E.F., Tice, R.R., and Behl, M. (2016). Neurite outgrowth in human induced pluripotent stem cell-derived neurons as a high-throughput screen for developmental neurotoxicity or neurotoxicity. NeuroToxicology *53*, 271–281.

Ryan, Scott D., Dolatabadi, N., Chan, Shing F., Zhang, X., Akhtar, Mohd W., Parker, J., Soldner, F., Sunico, Carmen R., Nagar, S., Talantova, M., et al. (2013). Isogenic human iPSC Parkinson's model shows nitrosative stress-induced dysfunction in MEF2-PGC1α transcription. Cell *155*, 1351–1364.

Ryssy, J., Prioste-Amaral, E., Assuncao, D.F., Rogers, N., Kirby, G.T., Smith, L.E., and Michelmore, A. (2016). Chemical and physical processes in the retention of functional groups in plasma polymers studied by plasma phase mass spectroscopy. Phys. Chem. Chem. Phys. *18*, 4496–4504.

Sarkar, A., Mei, A., Paquola, A.C.M., Stern, S., Bardy, C., Klug, J.R., Kim, S., Neshat, N., Kim, H.J., Ku, M., et al. (2018). Efficient generation of CA3 neurons from human pluripotent stem cells enables modeling of hippocampal connectivity in vitro. Cell Stem Cell *22*, 684–697.e689.

Schneider, C.A., Rasband, W.S., and Eliceiri, K.W. (2012). NIH Image to ImageJ: 25 years of image analysis. Nat. Methods *9*, 671–675.

Smith, L.E., Bryant, C., Krasowska, M., Cowin, A.J., Whittle, J.D., MacNeil, S., and Short, R.D. (2016). Haptotatic plasma polymerized surfaces for rapid tissue regeneration and wound healing. ACS Appl. Mater. Inter. *8*, 32675–32687.

Stenger, D.A., Pike, C.J., Hickman, J.J., and Cotman, C.W. (1993). Surface determinants of neuronal survival and growth on self-assembled monolayers in culture. Brain Res. *630*, 136–147.

Štrbková, L., Manakhov, A., Zajíčková, L., Stoica, A., Veselý, P., and Chmelík, R. (2016). The adhesion of normal human dermal fibroblasts to the cyclopropylamine plasma polymers studied by holographic microscopy. Surf. Coat. Technol. *295*, 70–77.

Tran, J., Anastacio, H., and Bardy, C. (2020). Genetic predispositions of Parkinson's disease revealed in patient-derived brain cells. NPJ Parkinson's Dis. *6*, 8.

Vadodaria, K.C., Mertens, J., Paquola, A., Bardy, C., Li, X., Jappelli, R., Fung, L., Marchetto, M.C., Hamm, M., Gorris, M., et al. (2016). Generation of functional human serotonergic neurons from fibroblasts. Mol. Psychiatry *21*, 49–61.

van den Hurk, M., and Bardy, C. (2019). Single-cell multimodal transcriptomics to study neuronal diversity in human stem cell-derived brain tissue and organoid models. J. Neurosci. Methods *325*, 108350.

Volpato, V., and Webber, C. (2020). Addressing variability in iPSC-derived models of human disease: guidelines to promote reproducibility. Dis. Model Mech. *13*, dmm042317.

Yamamoto, A., Mishima, S., Maruyama, N., and Sumita, M. (1998). A new technique for direct measurement of the shear force necessary to detach a cell from a material. Biomaterials *19*, 871–879.

Yamamoto, A., Mishima, S., Maruyama, N., and Sumita, M. (2000). Quantitative evaluation of cell attachment to glass, polystyrene, and fibronectin- or collagen-coated polystyrene by measurement of cell adhesive shear force and cell detachment energy. J. Biomed. Mater. Res. Part A *50*, 114–124.

Zabolocki, M., McCormack, K., van den Hurk, M., Milky, B., Shoubridge, A.P., Adams, R., Tran, J., Mahadevan-Jansen, A., Reineck, P., Thomas, J., et al. (2020). BrainPhys neuronal medium optimized for imaging and optogenetics in vitro. Nat. Commun. *11*, 5550.